Toward Improving Breast Cancer Imaging: Radiological Assessment of Propagation-Based Phase-Contrast CT Technology

Seyedamir Tavakoli Taba, Patrycja Baran, Sarah Lewis, Robert Heard, Serena Pacile, Yakov I. Nesterets, Sherry C. Mayo, Christian Dullin, Diego Dreossi, Fulvia Arfelli, Darren Thompson, Mikkaela McCormack, Maram Alakhras, Francesco Brun, Maurizio Pinamonti, Carolyn Nickson, Chris Hall, Fabrizio Zanconati, Darren Lockie, Harry M Quiney, Giuliana Tromba, Timur E Gureyev, Patrick C Brennan

Rationale and Objectives: This study employs clinical/radiological evaluation in establishing the optimum imaging conditions for breast cancer imaging using the X-ray propagation-based phase-contrast tomography.

Materials and Methods: Two series of experiments were conducted and in total 161 synchrotron-based computed tomography (CT) reconstructions of one breast mastectomy specimen were produced at different imaging conditions. Imaging factors include sample-to-detector distance, X-ray energy, CT reconstruction method, phase retrieval algorithm applied to the CT projection images and maximum intensity projection. Observers including breast radiologists and medical imaging experts compared the quality of the reconstructed images with reference images approximating the conventional (absorption) CT. Various radiological image quality attributes in a visual grading analysis design were used for the radiological assessments.

Results: The results show that the application of the longest achievable sample-to-detector distance (9.31 m), the lowest employed X-ray energy (32 keV), the full phase retrieval, and the maximum intensity projection can significantly improve the radiological quality of the image. Several combinations of imaging variables resulted in images with very high-quality scores.

Conclusion: The results of the present study will support future experimental and clinical attempts to further optimize this innovative approach to breast cancer imaging.

Key Words: Breast cancer; Radiological assessment; Computed tomography; Phase-contrast imaging; X-ray propagation-based imaging (PBI).

INTRODUCTION

Breast cancer is the most common type of cancer in women worldwide and one of the two leading causes of cancer death in women in both developing and developed countries (1). Breast screening programs are designed in different countries with the goal of early detection of breast cancer and currently two–dimensional (2D) mammography is the most common imaging modality (2) followed by clinical and imaging assessment of symptomatic or recalled patients (3). In developed countries, it has been shown that breast screening programs can reduce breast cancer mortality rates by about 20% (4). However, screening mammography has some diagnostic inefficiencies arising from the superimposition of breast tissue found with 2D imaging (5). Consequently, the average sensitivity of digital screening mammography is around 70% and its average specificity is close to 90% (6), showing considerable room for

improvement. There is also a potential risk from radiation exposures with screening mammography (7) and significant patient discomfort following breast compression (8). Digital breast tomosynthesis (DBT) and dedicated breast computed tomography (CT) are two more recent imaging technologies designed to help overcome the superimposition problems in 2D mammography. Data so far suggest there are advantages and disadvantages of DBT and CT compared to 2D mammography without significant reduction in dose (both techniques) and limited improvement of discomfort (DBT). For more discussion about these newer modalities see Alakhras et al (5) and Lindfors et al (9).

Most of clinically available X-ray-based breast imaging modalities exploit only X-ray attenuation information, which is based on the differences in absorption behavior of various soft tissues. With X-ray attenuation techniques, the soft-tissue contrast is not substantial because the differences in densities of different components of breast soft tissue are small. Phase-contrast imaging is an advanced X-ray imaging technology that can capture the refraction and phase shift of X-ray waves when they pass through objects (10−12). For high-energy X-ray beams, phase shift variations (the phase-contrast) can be considerably stronger than the attenuation contrast (13,14). Subsequently, being able to retrieve the phase shift of the X-ray beam shows a large potential for improving the quality of breast images. There are several phase-contrast imaging techniques including propagation-based imaging (PBI), analyzer-based imaging, crystal interferometry, edge illumination, and grating interferometry. Compared to all other phase-contrast techniques, PBI is experimentally the simplest way to exploit phase shift information because it does not require any X-ray optical elements between the sample and the detector. The optimum conditions of the PBI technique for its clinical applications are not known completely.

Synchrotron-based facilities are currently being used in an experimental form for advanced mammographic imaging of particularly challenging cases where conventional techniques have produced uncertain results. A pilot study of 2D phase-contrast mammography on patients has been carried at the SYRMEP beamline of Elettra (15,16). In the CT approach of PBI, the most effective use of phase information is made possible through image processing algorithms based on the Homogeneous Transport of Intensity equation (TIE-Hom) (17). The application of this method in breast CT allows to effectively reduce image noise, while preserving the edge sharpness in the images (18,19). In this framework, a program aiming to implement a PBI trial for breast CT, as a continuation of previous mammography clinical protocol, is ongoing at Elettra (20).

In order to help establish the optimum condition(s) for the practical application of PBI technique in breast cancer imaging, this study uses clinical/radiological evaluation and image perception by human observers for comparing the quality of images obtained at different imaging conditions. Rigorous radiological assessments and clinical evaluations are essential before any clinical trial and eventually clinical implementation of phase-contrast CT can happen.

A recent paper by Baran et al (21) defined some practical conditions of future live patient PBI by primarily analyzing objective image quality characteristics, such as spatial resolution and signal-to-noise ratio (SNR), as functions of imaging conditions and radiation dose. Baran et al's paper focused on physics of phase-contrast CT and objectively analyzed the 81 images that were subjectively assessed in stage I of this study. Our study provides complementary clinical evaluations that have not been previously undertaken with phase-contrast CT. We conducted the radiological assessments in two stages and in total 161 synchrotron-based CT reconstructions were clinically assessed. In stage I, we evaluated a set of 81 images that corresponded to a wide range of theoretical imaging conditions. Then, in stage II, we examined another set of 80 reconstructed images that represented a variation of subtler imaging conditions based on the data produced from stage I. All images in both stages were obtained from one mastectomy specimen. Based on the results of two series of experiments and rigorous radiological assessments using visual grading analysis (VGA), we showed that, under certain conditions, PBI leads to significant improvement in some important image quality attributes relevant to initial breast cancer diagnostics.

MATERIALS AND METHODS

Experimental Setups

The work reported here was performed according to the Directive 2004/23/EC of the European Parliament and of the Council of March 31, 2004 on setting standards of quality and safety for the donation, procurement, testing, processing, preservation, storage, and distribution of human tissues and cells. In addition, a written consent from the patient was obtained.

The X-ray phase-contrast CT scans were carried out at the SYRMEP beamline at the Elettra synchrotron, Trieste, Italy. The SYRMEP beamline is based on a bending magnet and provides a monochromatic, nearly parallel, laminar X-ray beam with an area of about 160 mm × 3 mm at a distance of 23 m from the source, at 30 keV (22). A Si (111) double-crystal monochromator was used in the Bragg configuration to deliver an X-ray beam in an energy range between 32 keV and 38 keV and an energy resolution of $\Delta E/E = 10^{-3}$. The detector used in this study was a Hamamatsu CMOS flat panel sensor C9252DK-14, which contains a CsI scintillator deposited directly on a 2D photodiode array. The detector was used in the partial scan mode with a pixel size of $100\ \mu m \times 100\ \mu m$.

A full coronal slice of one breast tissue specimen was used in all CT scans. This specimen was sampled during a surgical mastectomy from a 67-year-old woman. The sample was prepared for the experiment by being fixed in

formalin and sealed hermetically in a polyethylene bag. The transverse dimensions of the sample were 12 cm by 7.5 cm and its thickness was 4 cm. Histological examination of the sample showed invasive ductal carcinoma, moderately differentiated (grade 2) with solid-trabecular and focally lobular-like aspects. The maximum diameter of the tumor was 2.7 cm. Histological examination also showed multiple foci of intraductal papillomatosis and sclerosing adenosis, which are benign lesions. For each scan in this study, the number of CT projections was 1000, the angular range was 180° and the total exposure time was 40 seconds. An evaluation of delivered dose has been performed on the basis of the air kerma measured by the custom made ionization chambers realized for the patient trial (15). The assessment of Mean Glandular Dose was performed by applying a Monte Carlo method that simulated the standard breast composition (19) and considered an irradiation of the entire sample. The total Mean Glandular Dose was adjusted to be equal to or lower than the standard two-projection mammography or tomosynthesis (approximately 4 mGy).

Imaging Conditions

The five key PBI parameters examined in this study are listed in Table 1. In stage I, the CT scans were collected at three different sample-to-detector distances; 0.16 m (the smallest distance intended to approximate absorption-based CT), 1.85 m (distance corresponding to a maximum one reasonably achievable in most future clinical implementations), and 9.31 m (the longest distance accessible at SYRMEP) using three monochromatic X-ray energies: 32 keV, 35 keV, and 38 keV. These conditions were selected purposefully to allow statistical examination of interaction effects of different phase-contrast imaging parameters (23). In stage II, based on the results of stage one, imaging conditions were more optimized; 1.85 m and 9.31 m for sample-to-detector distances and 32 keV and 35 keV for X-ray beam energies.

With regard to CT reconstruction methods, iterative filtered back projection (iFBP) (24) and simultaneous iterative reconstruction technique (SIRT) with 400 and 1000 iterations (SIRT400 and SIRT1000) (25) were used in stage I to reconstruct the three-dimensional images of the breast tissue. In stage II, a wider range of CT reconstruction methods were assessed: iFBP, SIRT1000, equally sloped tomography (EST) (26), simple filtered back projection (FBP) and iterative total variation minimization reconstruction (iTV) (27).

A key quantity determining the physics of interaction of the X-ray incident beam with the sample is the complex refractive index (28), which can be presented as $n = 1 - \delta + i\beta$. The phase shift is determined by the real decrement (δ) and the absorption by the imaginary part (β) of the complex refractive index (13), as shown in Figure 1. In this study, a phase retrieval technique was used to exploit the phase shift information of the transmitted X-ray beam by applying the TIE-Hom algorithm to the projection data (17). Each CT reconstruction was performed at three levels of phase retrieval in stage I: full phase retrieval, half phase retrieval, and no phase retrieval. In the "full phase retrieval" case, δ/β ratios of close to the theoretical value (29) for glandular tissue relative to adipose tissue $((\delta_{gland} - \delta_{adipose})/(\beta_{gland} - \beta_{adipose}) = 870, 978,$ and 1083 for 32 keV, 35 keV, and 38 keV, respectively) were used. In "half phase retrieval," δ/β ratios equal to half the values in full phase retrieval were applied, while "no phase retrieval" case did not employ phase retrieval at all. In stage II, only full and half phase retrievals were used in combination with CT reconstructions.

Furthermore, the use of maximum intensity projection (MIP) was examined in stage II of the study. With maximum MIP, we are referring to standard image postprocessing technique, where a stack of several adjacent CT slices from the same 3-mm-thick reconstructed volume were processed together in such a way that the intensity of each pixel in the output image was set to the maximum value among the same pixels in each of the slices from the stack. Such a procedure tends to emphasize some subtle features in the image in a way that is somewhat complementary to median filtering. MIP is a standard tool in commercial radiological imaging

TABLE 1. List of Imaging Parameters Examined in This Study

Imaging Parameter	Description	Levels of Assessment in Stage I	Levels of Assessment in Stage II
Distance	Propagation (sample-to-detector) distance	0.16 m, 1.85 m, 9.31 m	1.85 m, 9.31 m
Energy	Energy of incident X-ray beam	32 KeV, 35 KeV, 38 KeV	32 KeV, 35 KeV
Reconstruction method	CT method used to reconstruct the 3D image	iFBP, SIRT400, SIRT1000	iFBP, SIRT1000, EST, FBP, iTV
Phase retrieval	Parameters of phase retrieval algorithm applied to individual projections	Full, half, without	Full, half
Maximum intensity projection (MIP)	Application of maximum intensity projection in postprocessing of the 3D image	No MIP	MIP, no MIP

CT, computed tomography; MIP, maximum intensity projection.
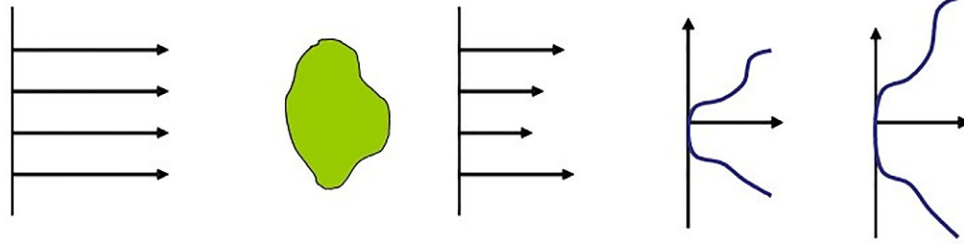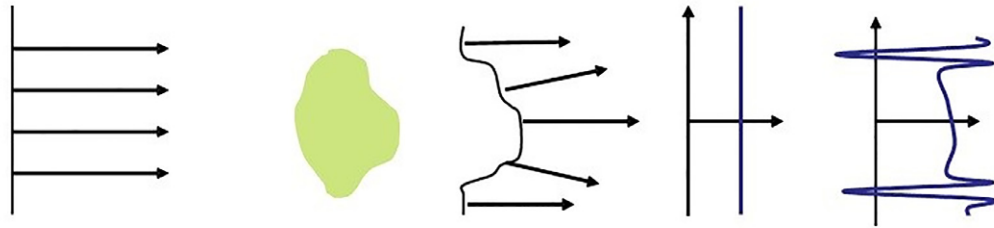
Figure 1. A schematic of an experimental setups of propagation-based imaging technique. Cross-sections of the intensity distribution in the "contact" and "phase-contrast" images are shown.

software and such images are well familiar to practicing radiologists.

X-TRACT (30) and STP (31) software were utilized for CT data analysis, which included preprocessing, phase retrieval, and CT reconstruction. In total, 81 images in stage I and 80 images in stage II were prepared for radiological assessments.

Radiological Assessments and Observers

The radiological assessments were based on the observation of selected regions of interest in single reconstructed slices. An experienced breast radiologist outlined the regions of interest on the images and we used VGA to perform the assessments. In a VGA study design, the observers rate their confidence about the fulfillment of certain attributes in the images. Six image quality attributes were selected by a group of experts to be used in the assessment. The images were evaluated in comparison to a reference image. In stage I, the imaging parameters for the reference image were chosen in a way that it provided an approximation to the standard absorption-based mammographic image. In stage II, the reference image was the image that received the highest radiological score in stage I among all images collected at the shortest propagation distance and without phase retrieval. The image quality attributes used the study and the imaging conditions of the reference images are shown in Figure 2. As indicated in this figure, 13 assessors in stage I and 15 assessors in stage II completed the radiological assessment task independently. Asses-

sors were a combination of breast specialist radiologists who were working for BreastScreen Australia and medical imaging experts who had diagnostic radiography qualifications and were widely involved in medical imaging and radiation sciences research. Each assessor had over 5 years' experience in working with radiologic images. The assessors rated each image quality attribute using a five-point scoring scale. The definition of scales was that the fulfillment of the attribute in the test image was clearly better than (+2); slightly better than (+1); equal to (0); slightly worse than (−1); and clearly worse than (−2) the fulfillment of the attribute in the reference image.

Statistical Analysis

For each assessor, we averaged the attribute scores of each image to summarize the overall quality score of that image. Before using the scores, we conducted an inter-rater reliability analysis to understand the level of agreement among individual assessors in rating images. Intraclass correlation coefficients (ICC) were used in this study for inter-rater reliability and agreement analysis (32,33). Moreover, we were interested in the level of agreement between two groups of assessors, namely radiologists and medical imaging experts, and ICC was also used to compare the average scores given by each group to each image. Finally, analysis of variance (ANOVA) was conducted to examine the effects of different imaging parameters (factors) and their interactions on the image quality. In stage I, we conducted a five-way factorial
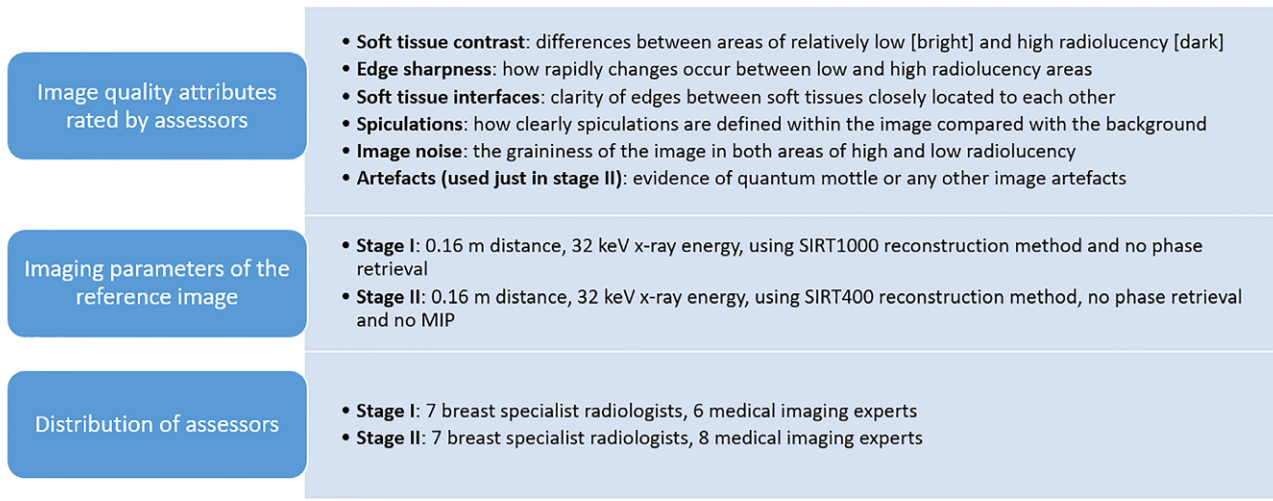
Figure 2. The design of the visual grading analysis (VGA) in stage I and stage II of the study.

ANOVA with four repeated measures factors (distance, energy, reconstruction method, and phase retrieval) and one between-subject factor (assessor group). Similarly, in stage II, a six-way factorial ANOVA with five repeated measures factors (distance, energy, reconstruction method, phase retrieval, and MIP) and one between-subject factor (assessor group) was conducted. SPSS software (version 22.0) was used for all statistical calculations.

Interpreting and presenting multi-factorial ANOVA results is complex. We have included the details of the wider ANOVA analysis as justification for our interpretations of the results. Readers will find the messages from the analysis fully summarized by the short accounts presented before the ANOVA results, and by inspecting the mean scores and shading in Tables 3 and 4.

between presented images at this stage. The level of agreement between radiologists and medical imaging experts was excellent in stage I and good in stage II. Furthermore, the ANOVA analysis indicated that in both stages there was no significant main effect of the assessor group on the image scores, $F(1, 11) = 0.136$, $p = .719$, and $F(1, 13) = 1.206$, $p = .292$, respectively.

In the next two subsections, the results of radiological assessments in the two stages of the study are presented. First, the mean quality scores and then the main effects and the interaction effects between various factors are shown. We caution that, although the main effects could describe a good "big picture" of the impacts of different factors on the image quality, they should be interpreted in conjunction with the interaction effects. Unless otherwise stated, all reported effects are statistically significant at $p \leq 0.001$.

RESULTS

Inter-rater Agreement and Between-Subjects Effect

The results of inter-rater agreements are reported in Table 2. It has been suggested in the literature that, as a rule of thumb, ICC values between 0.5 and 0.75 indicate moderate reliability, values between 0.75 and 0.9 indicate good reliability, and values greater than 0.90 indicate excellent reliability (33). In this study, the level of agreement among individual assessors was moderate in stage I and low in stage II. Lower agreement between assessors in stage II (compared to stage I) could be a result of subtler differences

Image Quality Assessments of Stage I

Table 3 presents a summary of the mean quality scores of different imaging conditions in stage I. The results showed that distance was the most important factor regarding image quality and all high-quality scores were at 9.31 m distance. Lower energy was more or less associated with higher quality score as well. Overall, images with phase retrieval had higher radiological quality than images with no phase retrieval. A key message revealed from the results was that, at maximum distance of 9.31 m and energies of 32 keV and 35 keV, several

TABLE 2. ICC Results Based on Two-Way Mixed Effects of Average Measures

Phase of the Study	Image Attributes	Intraclass Correlation	95% Confidence Interval	
			Lower Bound	Upper Bound
Stage I	ICC across all assessors	0.718	0.647	0.786
	ICC between two assessor groups	0.970	0.954	0.981
Stage II	ICC across all assessors	0.217	0.142	0.311
	ICC between two assessor groups	0.762	0.209	0.899

ICC, Intraclass correlation coefficients.

TABLE 3. The Mean Quality Scores of 81 Image Conditions in Stage I. The Scores Range From −2 to 2, Where a Higher Score Shows A Higher Image Quality. The Scores Below Zero Suggest Worse Image Quality Than the Reference Image. A Darker Highlight Color Shows a Higher Image Quality Than the Reference Image

Reconstruction Method	Level of Phase Retrieval	Distance Between Object and Detector								
		0.16 m			1.85 m			9.31 m		
		38 keV	35 keV	32 keV	38 keV	35 keV	32 keV	38 keV	35 keV	32 keV
iFBP	Without	-1.23	-1.02	-0.46	0.22	-0.51	0.71	-0.38	0.97	0.90
	Half	-0.77	-0.32	-0.03	0.98	0.34	0.09	1.58	1.85	1.80
	Full	-0.72	-0.42	-0.31	1.14	0.78	0.98	1.55	1.71	1.88
SIRT1000	Without	-0.88	-0.26	0.00	0.43	0.00	0.66	0.54	1.31	1.71
	Half	-0.78	-0.09	0.03	0.75	0.75	0.78	1.46	1.69	1.77
	Full	-0.85	-0.06	0.00	0.75	0.65	1.12	1.63	1.71	1.74
SIRT400	Without	-0.57	0.09	0.54	1.02	0.42	0.74	1.09	1.78	1.74
	Half	-0.42	0.37	0.31	1.02	1.02	1.02	1.34	1.72	1.80
	Full	-0.29	0.06	0.48	0.78	0.39	1.37	1.22	1.52	1.55

different combinations of reconstruction methods and phase retrievals could provide high-quality scores. The following section describes in detail the statistical analysis which supports this interpretation of the figures in Table 3.

The Main Effects (Stage I)
There was a significant main effect of the distance on the image quality score, $F(1.23, 13.54) = 150.23$. Post hoc tests revealed that the mean image quality score of the 9.31 m distance was significantly higher than the mean scores of 1.85 m and 0.16 m distances. The mean score of 1.85 m distance was also significantly higher than the mean score of 0.16 m distance. There was also a significant main effect of the energy on the image quality score, $F(2, 22) = 71.29$. Post hoc tests revealed that the mean score of 32 keV energy was significantly higher than the mean scores of 35 keV and 38 keV energies. The mean score of 35 keV energy was also significantly higher than the mean score of 38 keV energy.

The results showed a significant main effect of the phase retrieval on the image quality score, $F(1.19, 13.09) = 62.14$. Post hoc tests revealed that the mean scores of both half and full phase retrievals were significantly higher than the mean score of no phase retrieval. No difference between the mean scores of half and full phase retrievals was noted ($p = 1.000$). Finally, there was a significant main effect of the reconstruction method on the image quality score, $F(1.04, 11.47) = 9.67$, $p = .009$. Post hoc tests revealed that the mean score of SIRT400 method was significantly higher than the mean score of iFBP method ($p = .028$) and SIRT1000 method ($p = .015$). The mean score of SIRT1000 method was also higher than the mean score of iFBP method but the difference was not significant ($p = .060$).

The Interaction Effects (Stage I)
There was a significant interaction effect between the reconstruction method and the phase retrieval, $F(4, 44) = 40.12$.

Having half- or full phase retrievals reduced the effects of the reconstruction method on the image quality. This was to the extent that for full phase retrieval, the mean scores were more or less the same across different reconstruction methods. The quality score in iFBP method was highly dependent on the level of phase retrieval, but this dependency reduced for SIRT1000 and SIRT400 methods. This result is consistent with the difference in the nature of iFBP and SIRT algorithms: while iFPB does not include substantial implicit or explicit image smoothing in its implementation, the SIRT algorithm does. Image smoothing has somewhat similar effects to phase retrieval, therefore the effect of phase retrieval on the outcomes of SIRT reconstruction is not as a pronounced, as for the iFBP method. A significant interaction effect between the distance and the reconstruction method was also observed, $F(4, 44) = 9.15$. The dependence of quality score on the reconstruction method reduced with increased distance. Particularly, at 9.31 m distance, SIRT400 and SIRT1000 provided very similar quality scores while iFBP was slightly inferior. However, the performance of iFBP algorithm became comparable, or even superior to both SIRT algorithms, when the TIE-Hom phase retrieval (full or half) was included in the PCT reconstruction procedure.

The results showed that there was a significant interaction effect between the distance and the energy, $F(1.71, 18.80) = 20.99$. At higher distances, the effects of energy on the image quality were reduced. There was also another significant energy-based interaction effect, this time with phase retrieval, $F(4, 44) = 9.78$. The difference between having the phase retrieval and not having it was less for lower energies compared to higher energies. The latter conclusion, in particular, is consistent with the physics of phase-contrast imaging: the strength of phase-contrast compared to the absorption-contrast is a monotonically increasing function of the energy, within the studied energy range, for soft-tissue samples (28).

There was a significant interaction effect between the distance and the phase retrieval, $F(2.10, 23.18) = 5.70$, $p = .009$.

The dependence of quality score on the phase retrieval enlarged with increased distance. Indeed, by increasing the propagation distance one allows stronger phase-contrast effects to appear in the projection images, which, in turn, ensures that the subsequent phase retrieval improves the reconstructed image quality more strongly, compared to the conventional (absorption-only) images. Moreover, the interaction between the distance, the phase retrieval and the reconstruction method was showed to be a significant effect, $F(8, 88) = 9.53$. The combination effect of having phase retrieval (either half or full) and high distance, impacted the quality score of iFBP method more remarkably compared to the other reconstruction methods (which is consistent with our explanation of the difference in the nature of the two algorithms mentioned above).

There was a significant interaction effect between the distance, the energy and the phase retrieval, $F(8, 88) = 7.66$. The three-way interaction showed that, at energy of 38 keV and no phase retrieval, 1.85 m and 9.31 m distances resulted in almost the same mean quality scores. Finally, a significant interaction effect between the energy, the reconstruction method and the phase retrieval was observed, $F(8, 88) = 3.44$, $p = .002$. Having phase retrieval changed the relationship between the energy and the reconstruction method so that for higher phase retrieval, the dependence of quality score on the reconstruction method decreased, particularly for high energies.

Image Quality Assessments of Stage II

Table 4 presents a summary of the mean quality scores of different imaging conditions in stage II. Although the differences in image quality were subtler in this stage (because of more selective imaging conditions), the results reconfirmed the outputs of stage I by showing that higher distance and lower energy highly improved the image quality. As before,

details of the multifactorial ANOVA analysis are presented below in justification of this interpretation.

The Main Effects (Stage II)
There was a significant main effect of the distance on the image quality score, $F(1, 13) = 33.72$. Post hoc tests revealed that the mean quality score of the 9.31 m distance was significantly higher than the mean scores of 1.85 m distance. The results showed a significant main effect of the energy on the image quality score as well, $F(1, 13) = 59.56$. Post hoc tests revealed that the mean score of 32 keV energy was significantly higher than the mean scores of 35 keV energy. Furthermore, there was a significant main effect of the MIP on the image quality score, $F(1, 13) = 5.74$, $p = .032$. Post hoc tests revealed that the mean score of MIP was significantly higher than the mean score of no MIP. The results also showed a significant main effect of the phase retrieval on the image quality score, $F(1, 13) = 5.64$, $p = .034$. Post hoc tests revealed that the mean scores of full phase retrieval were significantly higher than the mean score of half phase retrieval. Finally, the results of stage II did not show any significant main effect of the reconstruction method on the image quality, $F(1.53, 19.92) = 1.80$, $p = .195$.

The Interaction Effects (Stage II)
There was a significant interaction effect between the distance and the energy, $F(1, 13) = 17.90$. Like stage I, this interaction effect showed that the dependence of image quality on the energy reduced at higher distances. The results also showed a significant interaction effect between the reconstruction method and the phase retrieval, $F(2.79, 36.27) = 7.34$. EST, FBP, and iFBP reconstruction methods presented higher image quality in conjunction with full phase retrieval while SIRT1000 worked

TABLE 4. The Mean Quality Scores Of 80 Image Conditions in Stage II.
The Scores Range From −2 to 2, Where a Higher Score Shows A Higher Image Quality. The Scores Below Zero Suggest Worse Image Quality Than the Reference Image. A Darker Highlight Color Shows a Higher Image Quality Than the Reference Image

Reconstruction Method	Level of Phase Retrieval	Distance Between Object and Detector							
		1.85 m				9.31 m			
		35 keV	35 keV	32 keV	32 keV	35 keV	35 keV	32 keV	32 keV
		No MIP	MIP	No MIP	MIP	No MIP	MIP	No MIP	MIP
EST	Half	0.33	0.14	0.47	0.79	0.52	1.00	0.88	1.00
	Full	0.34	0.42	0.71	0.87	0.99	1.17	1.29	1.37
FBP	Half	0.28	0.34	0.75	0.51	0.71	1.01	0.82	1.01
	Full	0.37	0.43	0.80	1.13	0.89	0.88	1.17	1.34
iFBP	Half	0.34	0.43	0.94	0.76	0.81	0.93	1.15	1.18
	Full	0.33	0.96	0.78	0.86	1.04	1.23	1.10	1.21
iTV	Half	0.17	0.73	0.79	0.87	0.61	1.24	0.96	1.24
	Full	0.59	0.48	0.88	0.99	0.69	0.99	0.98	1.10
SIRT1000	Half	0.54	0.38	0.86	0.71	0.94	1.09	1.11	1.07
	Full	0.34	0.08	0.87	0.80	0.73	0.86	0.87	1.17

better with half phase retrieval and iTV provided similar mean scores for full and half phase retrievals. Again, this is in agreement with our previous explanation that phase retrieval does not have a distinct impact on reconstruction methods that implement a substantial image smoothing. Furthermore, a significant interaction effect between the energy, the reconstruction method, and the phase retrieval was observed, $F_{(3.17, 41.21)} = 8.65$. The results revealed that at 32 keV energy, EST and FBP worked better with full phase retrieval while iFBP, Itv, and SIRT1000 provided approximately similar mean scores across two levels of phase retrieval. At 35 keV, however, all methods provided higher scores with full phase retrieval except for SIRT1000 which gave higher mean scores for half phase retrieval.

The interaction effect between the energy, the phase retrieval and the MIP was significant, $F_{(1, 13)} = 6.29$, $p = .026$. The results showed that when MIP and full phase retrieval were used, the impact of energy on the image quality increased. There was also a significant interaction effect between the reconstruction method and the MIP, $F_{(2.67, 34.69)} = 3.46$, $p = .031$. The results showed that all reconstruction methods provided higher image quality in conjunction with MIP except for SIRT1000, which was not impacted by this parameter. Moreover, there was a significant interaction effect between the reconstruction method, the phase retrieval and the MIP, $F_{(3.10, 40.24)} = 4.71$, $p = .006$. At both of MIP and no MIP, in general, EST, FBP, and iFBP worked better with full phase retrieval while SIRT1000 provided higher quality images with half phase retrieval. However, iTV provided higher mean score with full phase retrieval at no MIP and with half phase retrieval at MIP.

DISCUSSION

By means of two series of experiments and radiological assessments and statistical analysis, we showed that factors of distance, energy, reconstruction method, phase retrieval, and MIP had some effects on the image quality in propagation-based phase-contrast imaging, but these effects were of different magnitudes. The analysis also revealed that there are some important interaction effects among all these factors. Overall, the highest values in radiological quality scores were consistently achieved for images obtained at 9.31 m, the longest propagation distance in the study (Figure 3). This result is in complete accordance with the physics of the in-line PBI technique, which indicates that the SNR in the reconstructed image increases when propagation distance increases and TIE-Hom phase retrieval is used as part of the PCT image reconstruction (34). This escalation in the SNR is achieved mainly due to the exploitation of differences in the phase shift of X-ray wavefront across the sample (in addition to the absorption) and the reduction of X-ray scatter in the output image (35).

The results also showed that, for the considered sample, lower X-ray energy was related to higher image quality scores. Previous research demonstrates that the dependence of image quality on X-ray energy is not linear and a particular optimum energy exists that maximizes the SNR (23). This optimum energy depends on the imaging method, the

material composition, and the dimension of the sample and for a full-size breast tissue sample should be approximately between 30 keV and 40 keV. In stage I of this study, almost all high values in radiological quality scores were achieved at 32 keV or 35 keV energies. In stage II, we scrutinized the subtlety between these two and the results showed that, for the considered sample size and near-parallel monochromatic X-ray illumination, 32 keV could provide higher image quality. When considering future work, the variations in thickness and density of breast tissues will probably justify an adaptation of the X-ray energy but this would likely be within a relatively narrow range around the optimal energy that we have identified in this paper. Future studies should consider a wide range of breast sizes and densities to evaluate the optimum energies.

Previous research indicates that the application of the TIE-Hom phase retrieval algorithm in the PBI technique can decrease the impact of noise and increase the SNR in the reconstructed image, thus showing a large potential for improving the image quality (18,23). In a recent publication, Chou and Anastasio (36) have demonstrated that the application of the TIE-based phase retrieval leads to degradation of performance of a Hotelling observer for detecting a known signal in a known background, compared to the same method applied to raw propagation-based phase-contrast images. It is known that the generic TIE phase retrieval from images collected at two or more different propagation distances suffers from a strong numerical instability in the low spatial frequency region, see for example Gureyev et al (35). This instability typically results in strong low-frequency artifacts in the phase-retrieved images which can lead to deterioration of performance of numerical observer algorithms and to lower scores by human assessors. In contrast, the TIE-Hom phase retrieval algorithm (17) used in the present study is remarkably stable with respect to small errors and noise in the experimental image data and requires only a single propagation-based image for its application. It has also been shown (35) that even when the imaged object does not comply with the homogeneous-object approximation assumed in the TIE-Hom formalism, the reconstruction of the spatial distribution of the imaginary part of the complex refractive index remains remarkably accurate (unlike that of the real increment of the refractive index). Our previous theoretical (23) and experimental (19,35) studies, as well as publications by other groups, have demonstrated that the use of TIE-Hom method can significantly increase the SNR in the phase-retrieved images, without the obligatory deterioration in the spatial resolution that affects comparable low−pass-filtering techniques. The results from this study confirm this effect, showing that images obtained by the application of TIE-Hom phase retrieval had significantly higher radiological quality than images obtained with no phase retrieval.

One of the main contributions of this study is that it augments our understanding of how the TIE-Hom phase retrieval algorithm works in conjunction with different reconstruction methods. In both stages of the study, one of
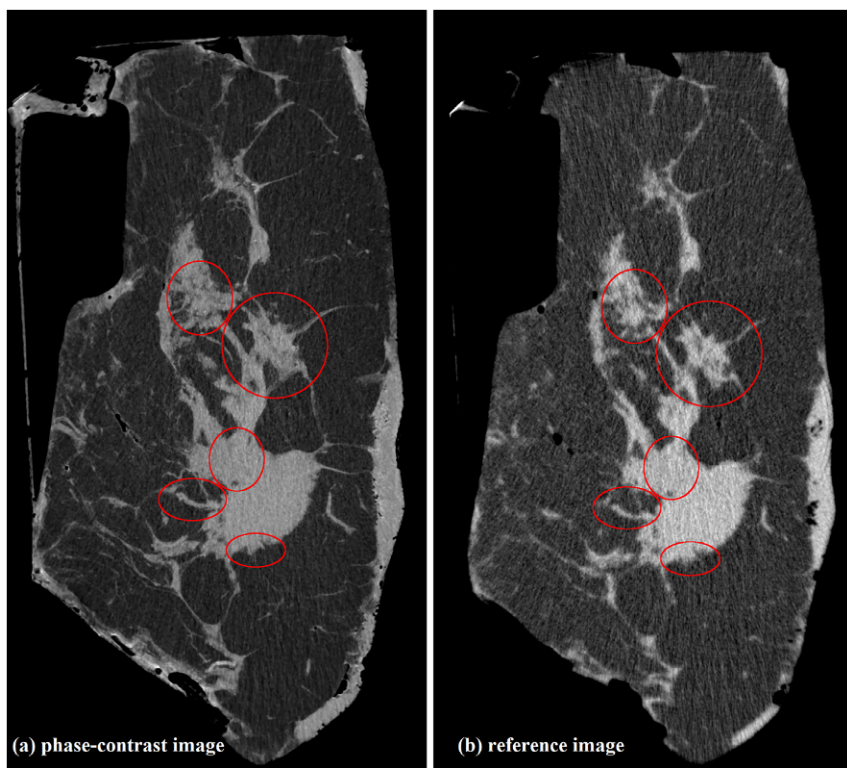
Figure 3. Two images of the breast tissue sample used in the radiological assessments at stage II of the study. Red ovals represent five regions of interest (ROIs) that were used for rating in the assessments. All images were collected at comparable Mean Glandular Dose equal or lower than 4 mGy. (a): A phase-contrast image with a high-quality score in radiological assessments (imaging condition: 9.31 m distance, 32 keV X-ray energy, using EST reconstruction method, full phase retrieval, and MIP). (b): The reference image, which represented an approximation to the conventional (absorption-based) mammographic image (imaging condition: 0.16 m distance, 32 keV X-ray energy, using SIRT400 reconstruction method, no phase retrieval, and no MIP) and obtained the highest radiological score in stage I among all absorption-based images. MIP, maximum intensity projection.

the most substantial interaction effects was found between the reconstruction method and the phase retrieval. Overall, application of phase retrieval increased the quality scores of EST, FBP, and iFBP methods more significantly compared to SIRT1000, SIRT400, and iTV methods. Thus, although different reconstruction methods were not substantially different across all imaging conditions, combination of full phase retrieval with EST, FBP, and iFBP outperformed other reconstruction methods, particularly at optimum conditions of high distances and lower energies.

The overall results showed the use of MIP was superior to no MIP although the application of MIP did not impact upon the quality score of the SIRT1000 reconstruction method. This outcome is consistent with the fact that the MIP method can be considered a type of image filtering, which affects less the images which are already substantially blurred, as in the case of SIRT1000 reconstructions.

In this study, while we examined a variety of exposure parameters such as energy and propagation distance, to facilitate assessment of specific parameters, we did this at the same or similar dose. Apart from the five key PBI parameters affecting the quality of resultant images that have been evaluated in the present work, other parameters such as the detector pixel size and resolution can also play an important role in PBI imaging. Analysis of these additional physical imaging parameters and their effect on objective image characteristics such as spatial resolution and contrast-to-noise ratio can be found in other publications, see for example Pacile et al (18), Nesterets et al (19), Longo et al (20), Baran et al (21), Tromba et al (22), Gureyev et al (34), and Gureyev et al (35).

The present study was deliberately performed on a single sample to allow the authors to accomplish an in-depth comparison of a variety of different imaging conditions for the same tissue. However, in order to establish the optimum conditions for PCT imaging of the breast, the results from this study should be considered in conjunction with the larger body of related work, which includes a variety of samples. Other experiments on a large number of samples indicate that the optimum conditions presented here can be used effectively for imaging typical whole breast samples. Earlier theoretical research and numerical simulations also support the results of this study (23,34).

With regards to future studies, we believe that the optimization performed in our study is applicable to a wide range of imaging systems based on synchrotron setups with near-parallel monochromatic X-ray beams (18−21). At the same time, substantial progress has been also achieved in recent years in the development of novel types of compact sources and microfocus generators (37,38), but further advances may still be necessary before these sources attain the performance characteristics required for clinical propagation-based CT imaging of live patients. The outcomes of our study can encourage the development of these future medical breast scanners employing X-ray phase-contrast and help with their design.

CONCLUSION

Before the clinical application of phase-contrast technology becomes possible in breast cancer imaging, the variables affecting the quality of images must be optimized through both objective estimation of physical quantities (such as spatial resolution and SNR) and subjective evaluation (image perception and cognition) of image attributes by human observers. The current study used a VGA paradigm to assess radiological quality of images obtained by phase-contrast PBI technique and demonstrated ways in which the PBI technique can be enhanced. In particular, long propagation sample-to-detector distance, sufficiently low X-ray energy beam, the application of MIP and correct level of application of TIE-Hom phase retrieval algorithm in conjunction with reconstruction methods were key parameters. The data presented should provide a good basis for future experimental and clinical protocols for further optimization of this novel and promising approach to breast imaging. Before any clinical trial of PBI technique, however, the results from this VGA study should be reinforced by receiver operating characteristic methodology so parameters such as sensitivity and specificity are fully explored. The receiver operating characteristic analysis is going to be at the center of the next stage of our studies. It will require the acquisition and evaluation of a large number of PBI CT scans of different mastectomy samples with a variety of breast cancer lesions, as well as imaging of cancer-free samples sourced from preventative breast surgeries (Fig 3).

DECLARATIONS OF INTEREST

None.

ACKNOWLEDGMENTS

REFERENCES

1. Ferlay J, Soerjomataram I, Dikshit R, et al. Cancer incidence and mortality worldwide: Sources, methods and major patterns in GLOBOCAN 2012. International Journal of Cancer. 2015; 136(5):E359–E386.
2. Albert U-S, Altland H, Duda V, et al. 2008 update of the guideline: early detection of breast cancer in Germany. Journal of Cancer Research and Clinical Oncology. 2009; 135(3):339–354.
3. Sztrókay A, Diemoz P, Schlossbauer T, et al. High-resolution breast tomography at high energy: a feasibility study of phase contrast imaging on a whole breast. Physics in Medicine and Biology 2012; 57(10):2931.
4. Marmot MG, Altman DG, Cameron DA, et al. The benefits and harms of breast cancer screening: an independent review. The Lancet 2012; 380 (9855):1778–1786.
5. Alakhras M, Bourne R, Rickard M, et al. Digital tomosynthesis: A new future for breast imaging? Clinical Radiology 2013; 68(5):e225–e236.
6. Pisano ED, Gatsonis C, Hendrick E, et al. Diagnostic Performance of Digital versus Film Mammography for Breast-Cancer Screening. New England Journal of Medicine 2005; 353(17):1773–1783.
7. Feig SA, Hendrick RE. Radiation risk from screening mammography of women aged 40−49 years. J Natl Cancer Inst Monogr 1997: 119–124.
8. Boone JM, Nelson TR, Lindfors KK, et al. Dedicated breast CT: radiation dose and image quality evaluation. Radiology 2001; 221:657–667. doi:10.1148/radiol.2213010334.
9. Lindfors KK, Boone JM, Nelson TR, et al. Dedicated Breast CT: Initial Clinical Experience. Radiology 2008; 246(3):725–733.
10. Coan P, Bravin A, Tromba G. Phase-contrast x-ray imaging of the breast: recent developments towards clinics. Journal of Physics D: Applied Physics 2013; 46(49):494007.
11. Keyrilainen J, Bravin A, Fernandez M, et al. Phase-contrast X-ray imaging of breast. Acta Radiol 2010; 51(8):866–884.
12. Taba ST, Gureyev TE, Alakhras M, et al. X-Ray Phase-Contrast Technology in Breast Imaging: Principles, Options, and Clinical Application. American Journal of Roentgenology 2018; 211(1):133–145.
13. Raupach R, Flohr T. Performance evaluation of x-ray differential phase contrast computed tomography (PCT) with respect to medical imaging. Med Phys 2012; 39:4761–4774. doi:10.1118/1.4736529.
14. Wu X, Liu H, Yan A. Optimization of X-ray phase-contrast imaging based on in-line holography. Nucl Instrum Methods Phys Res Sect B 2005; 234:563–572. doi:10.1016/j.nimb.2005.02.015.
15. Castelli E, Tonutti M, Arfelli F, et al. Mammography with Synchrotron Radiation: First Clinical Experience with Phase-Detection Technique. Radiology 2011; 259(3):684–694.
16. Fedon C, Rigon L, Arfelli F, et al. Dose and diagnostic performance comparison between phase-contrast mammography with synchrotron radiation and digital mammography: a clinical study report. Journal of medical imaging (Bellingham, Wash) 2018; 5(1):013503.
17. Paganin D, Mayo SC, Gureyev TE, et al. Simultaneous phase and amplitude extraction from a single defocused image of a homogeneous object. J Microsc 2002; 206:33–40.
18. Pacile S, Brun F, Dullin C, et al. Clinical application of low-dose phase contrast breast CT: methods for the optimization of the reconstruction workflow. Biomed Opt Express 2015; 6(8):3099–3112.
19. Nesterets YI, Gureyev TE, Mayo SC, et al. A feasibility study of X-ray phase-contrast mammographic tomography at the Imaging and Medical beamline of the Australian Synchrotron. J Synchrotron Radiat 2015; 22 (6):1509–1523.
20. Longo R, Arfelli F, Bellazzini R, et al. Towards breast tomography with synchrotron radiation at Elettra: first images. Phys Med Biol 2016; 61 (4):1634–1649.
21. Baran P, Pacile S, Nesterets YI, et al. Optimization of propagation-based x-ray phase-contrast tomography for breast cancer imaging. Phys Med Biol 2017; 62(6):2315–2332.
22. Tromba G, Longo R, Abrami A, et al. The SYRMEP Beamline of Elettra: Clinical Mammography and Bio-medical Applications. AIP Conference Proceedings 2010; 1266(1):18–23.
23. Nesterets YI, Gureyev TE. Noise propagation in x-ray phase-contrast imaging and computed tomography. J Phys D Appl Phys 2014; 47:105402.
24. Myers GR, Thomas CDL, Paganin DM, et al. A general few-projection method for tomographic reconstruction of samples consisting of several distinct materials. Appl Phys Lett 2010; 96:021105.
25. Van der Sluis A, van der Vorst HA. SIRT-and CG-type methods for the iterative solution of sparse linear least-squares problems. Linear Algebra Its Appl 1990; 130:257–303.
26. Miao J, Förster F, Levi O. Equally sloped tomography with oversampling reconstruction. Phys Rev B 2005; 72:052103.
27. Ludwig R, Frank B, Christof F, et al. Improved total variation-based CT image reconstruction applied to clinical data. Phys Med Biol 2011; 56:1545.
28. Wilkins SW, Nesterets YI, Gureyev TE, et al. On the evolution and relative merits of hard X-ray phase-contrast imaging methods. Philosophical

Transactions of the Royal Society of London A: Mathematical, Physical and Engineering Sciences 2014; 372(2010).

29. TS-Imaging Website. www.ts-imaging.net/Services/Simple/ICUtilXdata.aspx; 2016 (Accessed: 9 September 2016).

30. Gureyev TE, Nesterets Y, Ternovski D, et al. Toolbox for advanced X-ray image processing. SPIE Optical Engineering+ Applications: International Society for Optics and Photonics 2011. 81410B-B-14.

31. Brun F, Pacilè S, Accardo A, et al. Enhanced and flexible software tools for X-ray computed tomography at the Italian synchrotron radiation facility Elettra. Fundamenta Informaticae 2015; 141(2-3):233–243.

32. LeBreton JM, Senter JL. Answers to 20 Questions About Interrater Reliability and Interrater Agreement. Organ Res Methods 2008; 11:815–852. doi:10.1177/1094428106296642.

33. Koo TK, Li MYA. Guideline of selecting and reporting intraclass correlation coefficients for reliability research. J Chiropractic Med 2016; 15:155–163. doi:10.1016/j.jcm.2016.02.012.

34. Gureyev T, Mayo S, Nesterets YI, et al. Investigation of the imaging quality of synchrotron-based phase-contrast mammographic tomography. Journal of Physics D: Applied Physics 2014; 47(36):365401.

35. Gureyev T, Mohammadi S, Nesterets Y, et al. Accuracy and precision of reconstruction of complex refractive index in near-field single-distance propagation-based phase-contrast tomography. J Appl Phys 2013; 114:144906.

36. Chou, C-Y & Anastasio, MA in SPIE Medical Imaging 2016: Physics of Medical Imaging. 97835J-97835J-97836 (International Society for Optics and Photonics).

37. Bech M, Bunk O, David C, et al. Hard X-ray phase-contrast imaging with the Compact Light Source based on inverse Compton X-rays. Journal of Synchrotron Radiation 2009; 16(1):43–47.

38. Larsson DH, Takman PAC, Lundström U, et al. A 24 keV liquid-metal-jet x-ray source for biomedical applications. Review of Scientific Instruments 2011; 82(12):123701.